JCI The Journal of Clinical Investigation

Small molecule JQ1 promotes prostate cancer invasion via BET-independent inactivation of FOXA1

Leiming Wang, … , Sophia Y. Tsai, Ming-Jer Tsai

J Clin Invest. 2019. https://doi.org/10.1172/JCI126327.

Research In-Press Preview **Oncology**

Graphical abstract

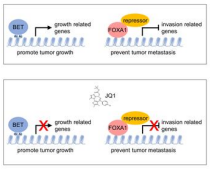

Small molecule JQ1 promotes prostate cancer invasion via BET-independent inactivation of FOXA1

Leiming Wang[1], Mafei Xu[1], Chung-Yang Kao[1], Sophia Y. Tsai[1,2,*], Ming-Jer Tsai[1,2,*]

[1] Department of Molecular and Cellular Biology, Baylor College of Medicine, Houston, Texas 77030, USA. [2] Department of Medicine and Program in Developmental Biology, Baylor College of Medicine, Houston, Texas 77030, USA

* Correspondence: stsai@bcm.edu (S.Y.T.), mtsai@bcm.edu (M.J.T.)

Sophia Y. Tsai

Department of Molecular and Cellular Biology, Baylor College of Medicine

One Baylor Plaza, BCM130, Houston, Texas 77030, USA

Phone: 713-798-6251 and E-mail: stsai@bcm.edu

Ming-Jer Tsai

Department of Molecular and Cellular Biology, Baylor College of Medicine

One Baylor Plaza, BCM130, Houston, Texas 77030, USA

Phone: 713-798-6253 and E-mail: mtsai@bcm.edu

The authors have declared that no conflict of interest exists.

Abstract

Recent findings have shown that inhibitors targeting BET (bromodomain and extraterminal domain) proteins, such as the small molecule JQ1, are potent growth inhibitors of many cancers and hold promise for cancer therapy. However, some reports also have revealed that JQ1 can activate additional oncogenic pathways and may affect EMT (epithelial mesenchymal transition). Therefore, it is important to address the potential unexpected effect of JQ1 treatment, such as cell invasion and metastasis. Here, we showed that in prostate cancer, JQ1 inhibited cancer cell growth but promoted invasion and metastasis in a BET protein independent manner. Multiple invasion pathways including EMT, BMP (bone morphogenetic protein) signaling, chemokine signaling and focal adhesion pathway were activated by JQ1 to promote invasion. Notably, JQ1 induced upregulation of invasion genes through inhibition of FOXA1, an invasion suppressor in prostate cancer. JQ1 directly interacted with FOXA1, inactivated FOXA1 binding to its interacting repressors, TLE3, HDAC7 and NFIC, thus blocking FOXA1 repressive function and activating the invasion genes. Our finding indicates that JQ1 has an unexpected effect of promoting invasion in prostate cancer. Thus, the ill effect of JQ1 or its derived therapeutic agents cannot be ignored during cancer treatment, especially in FOXA1 related cancers.

Introduction

Prostate cancer is the most commonly diagnosed cancer in men, and the second leading cause of cancer-related death in most western countries. Due to the crucial roles of androgen receptor (AR) in prostate cancer progression, androgen deprivation therapy (ADT) by surgical or chemical castration remains the major treatment regimen (1). However, the response is transient, and most patients develop resistance to ADT and progress to castration-resistant prostate cancer (CRPC) with high mortality (2). AR antagonists such as Bicalutamide and Enzalutamide were then developed to treat CRPC patients (3). Unfortunately, some unwanted effects are associated with treatment of these AR antagonists, including increased cancer metastasis and neuroendocrine differentiation (4-6), eventually leading to treatment failure. Thus, identification of novel treatment approaches and therapeutic targets becomes imperative to benefit prostate cancer patients.

Epigenetic-based therapies are becoming more and more promising for cancer treatment. BET (bromodomain and extraterminal domain) proteins are a family of epigenetic regulators, which include three ubiquitously expressed bromodomain-containing proteins BRD2, BRD3 and BRD4, and the testis-specific BRDT. Through their two acetylated lysine binding bromodomains and unique ET domain, BET proteins read acetylated histones and interact with histone modifiers as well as transcription factors to regulate gene transcription in different physiological conditions and diseases (7-9). Based on their essential roles in oncogene transcription and their upregulation in multiple cancers, targeting BET proteins has been considered as a novel cancer treatment strategy (10). Small molecule inhibitors targeting BET proteins (i-BET), such as JQ1, were identified to reversibly bind to bromodomains, disrupt the association of BET proteins with acetylated lysine in histones and transcription factors, repress oncogene expression, and eventually lead to cessation of cancer cell growth (8, 11, 12). In fact, i-BETs have emerged as an exciting new epigenetic therapeutic strategy for multiple cancers,

especially for advanced aggressive cancer types, such as CRPC, TNBC (Triple-negative breast cancer) and NUT (nuclear protein in testis) midline carcinoma (11-13). However, some reports recently suggest that JQ1 may also have unexpected effects. JQ1 affects both BET protein dependent and independent transcription regulation, and regulates distinct pathways upon continued treatment (14). JQ1 also induces variable oncogenic pathway responses in ovarian cancer cells (15). BET proteins exhibit transcriptional and functional opposition in EMT (epithelial to mesenchymal transition) (16), raising a possibility that JQ1 may promote EMT and metastasis.

Here, we show that BET protein inhibitor JQ1 suppressed prostate cancer cell proliferation but promoted invasion and metastasis independent of BET proteins. JQ1 directly interacted with FOXA1 and promoted invasion through inhibition of FOXA1 to activate multiple invasion pathways, including BMP signaling and EMT. Our study strongly suggests that more attention should be focused on the potential unexpected effects of JQ1 or JQ1 derived inhibitors. It also implies that combination treatment strategies could be used to overcome the potential metastatic promoting effect of JQ1.

Results

JQ1 promotes prostate cancer cell invasion

To examine the effect of JQ1 on prostate cancer cell growth and invasion, we first determined the functional concentration of JQ1. JQ1 inhibited prostate cancer cell growth in a dose dependent manner, with an IC50 of about 200 nM on LNCaP, C4-2 and 22Rv1 cells (Supplemental Figure 1A). Cells treated with 200 nM JQ1 showed a significant growth inhibition (Supplemental Figure 1B). Interestingly, we observed obvious JQ1 induced changes in cell morphology. JQ1 treated cells appeared to be astrocyte-like, with fusiform or fibroblastic

phenotypes, characteristic of mesenchymal cells with elongated and more leading-edge protrusions (Figure 1A). This morphological change raises the possibility that JQ1 treatment may enhance cell invasion. Indeed, a time- and dose-dependent increase in cell invasion was observed in multiple prostate cancer cells after JQ1 treatment (Figure 1B, 1C and Supplemental Figure 1C). To further evaluate the effect of JQ1 on invasion, we examined additional JQ1 derived inhibitors. After assessing their functional concentration that could suppress c-Myc expression and reduce cell proliferation (Supplemental Figure 1D and E), we found that all JQ1 derived inhibitors, including I-BET762, I-BET151 and OTX015, promoted cell invasion (Figure 1D). In accordance with increased protrusions and invasion, JQ1 significantly enhanced formation of focal adhesions that are crucial for cell migration and invasion (Supplemental Figure 1F). Moreover, through tail vein injection of luciferase-labeled prostate cancer cells, we measured JQ1 affected metastasis in mice. JQ1 did not alter either the expression of luciferase driven by a CMV promoter on a lentiviral vector in cells or luciferase activity (Supplemental Figure 1G and H). Importantly, JQ1 injection resulted in enhanced homing of luciferase-labeled cells into typical prostate cancer metastasized organs such as lymph nodes and bone as well as other sporadic sites (Figure 1E and Supplemental Figure 1I), indicating that JQ1 promoted prostate cancer cell metastasis. Moreover, JQ1 treatment in this metastatic mouse model led to poor survival in comparison to the vehicle treated control (Supplemental Figure 1J). We further used a prostate cancer transgenic mouse model (probasin-Cre driven *Pten* null mice) to address whether JQ1 increases metastasis in this mouse model. We measured prostate cancer cell metastasis to the draining lumbar lymph nodes through immunohistochemistry detection of AR positive prostatic cells in lymph nodes. AR protein levels were not increased by JQ1 (Supplemental Figure 1K), analogous to previous reports (11, 17). However, we found that the number of AR positive cells in the draining lumbar lymph nodes was increased after JQ1 treatment (Figure 1F, G and H), indicating enhanced

prostate cancer cell metastasis to lymph nodes. Taken together, these results indicate that JQ1 promotes invasion and metastasis of prostate cancer.

JQ1 activates invasion pathways

To dissect the molecular events of JQ1 promoted invasion, we performed transcriptome profiling by RNA-sequencing of JQ1 treated cells (Supplemental Figure 2A). Gene Ontology analysis revealed that a JQ1 upregulated gene profile was associated with biological processes such as cell migration and endocytosis, while a downregulated gene profile was associated with cell cycle and transcription (Supplemental Figure 2B). We further performed GSEA (Gene Set Enrichment Analysis) to analyze enriched hallmarks and pathways upon JQ1 treatment (Supplemental Figure 2C and D). In the top enrichment list, multiple invasion pathways were activated by JQ1, such as TGFβ family signaling, EMT, chemokine signaling, focal adhesion and actin cytoskeleton regulation (Figure 2A). Many key invasion genes in these pathways were confirmed to be upregulated by JQ1 treatment (Figure 2B).

The typical role of JQ1 in prostate cancer is to block BET proteins and AR signaling. Interestingly, JQ1 promoted invasion is unrelated to blocking BET proteins or AR, because knockdown of single BET, all BET, or AR did not promote invasion (Figure 2C and Supplemental Figure 3A). In fact, when all BET proteins were suppressed, there was a decrease in cell invasion ability, yet JQ1 still promoted invasion in the absence of all BET proteins (Figure 2D). Likewise, we found that knockdown of all BET proteins did not phenocopy JQ1 in activating invasion/EMT genes, while JQ1 activated most invasion/EMT genes in the absence of all BET proteins (Figure 2E and Supplemental Figure 3B). Consistently, knockdown of BRD4, the key BET protein, regulated distinct pathways compared to JQ1 (Supplemental Figure 4A), and JQ1 still activated similar invasion pathways including TGFβ family signaling and EMT regardless of BRD4 expression level (Supplemental Figure 4B).

Taken together, these results suggest that JQ1 promotes prostate cancer invasion in a BET protein independent manner.

To determine whether JQ1 activated invasion pathways contribute to enhanced invasion, we investigated TGFβ family signaling as it plays crucial roles in promoting EMT and cancer cell invasion. We found Smad1/5 phosphorylation was significantly increased by JQ1 treatment (Figure 3A), suggesting TGFβ family member BMP signaling was activated. Similar results on JQ1 promoting Smad1/5 phosphorylation were obtained in multiple prostate cancer cells (Figure 3B). A time dependent increase of phosphorylated Smad1/5 as well as AKT, a kinase that can be activated by BMP, was further observed after JQ1 treatment (Figure 3A and Supplemental Figure 5A). In addition, GSEA analysis showed that the response to BMP (GO:0071772) signature was positively enriched in JQ1 treated cells (Figure 3C). Moreover, we found that multiple JQ1 derived inhibitors all activated BMP signaling and promoted expression of mesenchymal marker *VIM* (Supplemental Figure 5B and 5C), which is consistent with the role of BMP signaling in promoting EMT in cancer cells.

We further investigated the role of BMP signaling in JQ1-promoted invasion. Through BMP signaling inhibitor LDN-212854, we found that blocking BMP signaling significantly impaired upregulation of JQ1 activated invasion genes and EMT marker *VIM* (Figure 3D), suggesting BMP signaling might play an important role in JQ1-promoted invasion. As expected, blocking BMP signaling either through LDN-212854 or siRNA against BMP receptors, ALK1/2/3, significantly impaired JQ1-promoted invasion (Figure 3E, F, G, H and Supplemental Figure 5D). Next, we asked whether JQ1 induced BMP signaling identified in cultured cells has any relevance to prostate cancer patients. Notably, we found 173 JQ1-induced BMP target genes whose signature was enriched in metastatic prostate cancer tissues as compared to primary cancer tissues (Figure 3I), supporting that BMP signaling plays a role in prostate cancer

metastasis. Taken together, our results indicate that JQ1-activated BMP signaling plays an important role in JQ1-promoted invasion.

JQ1 inhibits FOXA1 to promote prostate cancer cell invasion

To determine how JQ1 activates invasion pathways and genes, we searched for responsible transcription factors that have binding sites on the promoter of JQ1-activated invasion genes using the oPOSSUM program (18). We predicted a list of transcription factors that have potential binding sites on the promoter of 114 JQ1-activated invasion genes (Supplemental Figure 6A). Taking into account the expression levels of these transcription factors in cells (Supplemental Figure 6B), FOXA1 was highlighted as a promising candidate. Subsequently, we found that JQ1-activated invasion genes were negatively regulated by FOXA1 (Figure 4A). Importantly, not only these invasion genes, but JQ1's regulated gene profile was also negatively regulated by FOXA1 (Figure 4B), indicating that JQ1 indeed inhibits FOXA1 activity. Interestingly, many BMP ligands and receptors which contribute to BMP signaling activation were upregulated by JQ1 (Supplemental Figure 6C). FOXA1 also ranked as the top candidate of responsible transcription factors for JQ1 activated BMP ligands and receptors (Supplemental Figure 6D and 6E). Furthermore, FOXA1 indeed negatively regulated BMP ligands and receptors as well as BMP signaling marker *ID1* (Supplemental Figure 6F), further supporting that JQ1 inhibits FOXA1 in prostate cancer cells.

In addition, we compared JQ1 induced reduction of FOXA1 activity and BET protein activity. The activity was indicated by the expression of specific target genes regulated by FOXA1 or BRD2/3/4 (Supplemental Figure 7A). We found that the dosages of JQ1 in inhibition of FOXA1 and BRD2/3/4 specific target gene expression were similar (Supplemental Figure 7B), reinforcing that JQ1 inhibits FOXA1 as well as BET activity. Moreover, JQ1 inhibited FOXA1 activity and promoted invasion in a similar time dependent manner (Supplemental Figure 7C

and Figure 1B). Consistent to the repressive role of FOXA1 in JQ1-activated invasion genes, we found a negative correlation between *FOXA1* and JQ1-activated invasion genes in human prostate cancer tissues (Figure 4C). Moreover, in the absence of FOXA1, genes important for invasion were upregulated and JQ1 failed to further activate the expression of these invasion genes in most cases (Figure 4D), reinforcing that JQ1 inhibits FOXA1 activity to activate invasion genes. Likewise, we found FOXA1 knockdown promoted invasion, and JQ1 failed to further promote invasion when FOXA1 was repressed (Figure 4E). Together, these results indicate that JQ1 inhibits FOXA1 to activate invasion genes and promote invasion.

JQ1 interacts with FOXA1 and inhibits FOXA1 binding to repressors

Subsequently, we investigated how JQ1 inhibits FOXA1 to activate invasion genes. FOXA1 protein levels were largely not affected by JQ1 treatment (Supplemental Figure 8A). Therefore, we speculated that JQ1 might interact with FOXA1 to block FOXA1 invasion suppressor function. The result of cellular thermal shift assays (CETSA) supported that JQ1 bound to FOXA1 and led to significant thermal stabilization of FOXA1 (Figure 5A). Indeed, through biotinylated JQ1 pull-down assays, we found that JQ1 interacted with both overexpressed Flag tagged FOXA1 and endogenous FOXA1 in cell lysate as well as purified FOXA1 protein (Figure 5B, C and D). These results indicate that JQ1 interacts with FOXA1 directly.

Next, we asked whether binding of JQ1 affects the binding of FOXA1 to its target genes using ChIP assays. As shown in Supplemental Figure 8B, we did not observe apparent reduction of FOXA1 binding to the promoter of its target invasion genes upon JQ1 treatment. Since FOXA1 is known to recruit co-repressors and co-activators to regulate gene expression, we speculated that through interaction with FOXA1, JQ1 might disrupt FOXA1 binding to repressors, which leads to re-expression of FOXA1 repressed invasion genes and promotes cellular invasion ability. Among FOXA1 interacting proteins, TLE3 (19, 20), HDAC7 (21) and NFIC (22) have

been shown to have FOXA1 co-repressor function and are implicated in cell invasion regulation. We found that these repressors were involved in regulation of invasion genes that were repressed by FOXA1 (Supplemental Figure 8C and D). Knockdown of these repressors promoted expression of FOXA1 repressed invasion genes, while silencing of FOXA1 failed to further induce upregulation of invasion genes in the absence of these repressors (Supplemental Figure 8E), indicating that TLE3, HDAC and NFIC play a role in FOXA1 induced repression of these invasion genes. Importantly, JQ1 inhibited FOXA1 binding to the repressors, such as TLE3, HDAC7 and NFIC (Figure 5E), resulting in a reduction of recruitment of these repressors to FOXA1 binding sites on the promoters of the invasion genes (Figure 5F) as assayed by ChIP-qPCR. Moreover, in the absence of TLE3, HDAC7 and NFIC, JQ1 failed to further increase the expression of invasion genes (Figure 5G and Supplemental Figure 9A). Our results suggest that JQ1 interacts with FOXA1 to inhibit FOXA1 binding to co-repressors, thus allowing the expression of FOXA1 repressed genes that are important for invasion and metastasis. In addition, not only was JQ1 capable of reducing binding of repressors to FOXA1, JQ1 could also reduce the protein levels of TLE3, HDAC7 and NFIC in multiple prostate cancer cell lines (Supplemental Figure 9B). JQ1 might reduce protein levels through regulating their protein stability (Supplemental Figure 9C and D). Taken together, our results indicate that JQ1 inhibits FOXA1's repressive activity by interacting with FOXA1 to disrupt its binding to co-repressors, thus allowing for the re-expression of genes important for invasion.

Discussion

Recently, inhibitors that target BET proteins, such as JQ1, have been shown to be a promising drug for many types of cancer (10, 12). In response to JQ1 treatment, c-Myc expression and AR activity are reduced in prostate cancer, leading to growth inhibition (11). However, it also

has been shown that JQ1 may have unexpected effects on cancer metastasis, which is lethal for cancer patients (15, 16). In this study, we show that JQ1 interacted with FOXA and inhibited the repressor function of FOXA1 to enhance the expression of genes important for invasion, thus promoting prostate cancer metastasis.

JQ1 has been shown to bind to the bromodomains of BET proteins with a Kd of about 50-190 nM, and inhibits binding of acetylated histone H4 peptide to BRD4 with IC50 values of 77 and 33 nM for the two bromodomains (12). It has also been reported that potent biological effects of JQ1 are observed at 50-100 nM (23), and many cancer cells, including prostate cancer cells, respond to JQ1 with IC50 values under 300 nM (11, 13). However, some cancer cells were treated with a much higher dosage of JQ1 in some reports. Here, we chose 200 nM JQ1 for prostate cancer cell treatment to minimize the off-target toxicity. We also administered JQ1 for a longer time period, up to 3 days, to mimic prolonged clinical treatment. JQ1 at 200 nM was effective and sufficient to inhibit cell proliferation and reduce c-Myc expression. We found that invasion of multiple prostate cancer cell lines was promoted by JQ1 as well as its derived inhibitors. In addition, we showed that knockdown of BET proteins or AR did not promote invasion, indicating that JQ1 may promote invasion through other mechanisms. Consistent with our observation, it has been shown that JQ1 induces variable oncogenic pathways independent of BET protein's role in transcriptional regulation (14, 15).

Cancer metastasis promotion appears to be a concern for cancer growth inhibition drugs. For example, chemotherapy has been shown to induce cancer metastasis through a tumor-metastasis-receptive microenvironment (24, 25). Targeted therapy such as epigenetic HDAC inhibitors has also been found to promote EMT and metastasis in multiple cancers (26). In addition, the prostate cancer specific drug Enzalutamide has been revealed to induce EMT and promote metastasis (27). Through GSEA analysis of the JQ1 regulated gene profile, we found that JQ1 activated multiple invasion pathways in prostate cancer, including EMT, TGFβ family

signaling, chemokine signaling, focal adhesion, and actin cytoskeleton regulation. EMT, which plays a crucial role in drug-induced metastasis, is a cellular process defined by the loss of epithelial characteristics of tight cell-cell adhesion and apico-basal polarization and the gain of mesenchymal characteristics of motility and invasion. EMT renders cancer cells to become more migratory and resistant to drug treatment, thus eventually leading to enhanced cancer metastasis (28). In this study, we showed that administration of JQ1 to multiple prostate cancer cell lines resulted in EMT, in which BMP signaling was activated. BMPs, members of the TGFβ family, are key inducers of EMT that contribute to metastasis of multiple cancer types, including prostate cancer (29, 30). Interestingly, we showed that treatment with BMP signaling inhibitor, LDN-212854, significantly impaired JQ1 induced cell invasion and expression of some EMT pathway genes. Taking into account that EMT might contribute to JQ1 resistance that was observed in multiple cancer cells (13, 31, 32), it is foreseeable that combination treatment with BMP inhibitors might be applicable for future cancer treatment.

JQ1 promoted invasion genes have potential binding sites for Fork-head box proteins. Among them, FOXA1 (Fork-head box protein A1), a winged-helix transcription factor, was the top predicted transcription factor that is highly expressed in prostate cancer. Moreover, FOXA1 is essential for prostate organogenesis, and plays important roles in prostate cancer development (33, 34). Validation results showed that FOXA1 was responsible for inhibiting the expression of JQ1-induced invasion genes. In addition, we found that many JQ1-activated BMP ligand and receptor genes were also repressed by FOXA1. Moreover, the FOXA1 signature was negatively enriched in the JQ1 regulated gene profile, supporting that JQ1 indeed represses FOXA1 activity. Although JQ1 is a BET protein inhibitor, our data clearly showed that it did not work through BET proteins to exert its effect on invasion and metastasis. Instead, it interacted directly with FOXA1 and hindered FOXA1's ability to repress the expression of genes critical for invasion and metastasis.

FOXA1 is regarded as a pioneer factor that binds to condensed chromatin and opens chromatin to facilitate subsequent recruitment of other transcription factors and regulators (35, 36). FOXA1 plays important roles in prostate cancer, because FOXA1 recruits AR to regulate genes crucial for prostate cancer cell growth (35, 37). Therefore, blocking FOXA1 reduces AR transcription activity to inhibit prostate cancer cell growth. Furthermore, FOXA1 is a maintenance factor for the epithelial cell phenotype, and exhibits inhibitory activity on EMT and cancer metastasis in prostate, breast and pancreatic cancer (38-41). FOXA1 represses transcription of genes in cell motility, EMT and neuroendocrine differentiation in prostate cancer though an AR-independent mechanism (42, 43). Consistent with increasing evidence that FOXA1 promotes prostate cancer cell proliferation but prevents metastasis, our findings indicate that through inhibition of FOXA1, JQ1 blocks prostate cancer proliferation but enhances metastasis.

A variety of FOXA1 interacting partners have been shown to confer AR dependent and independent roles of FOXA1 in prostate cancer, which may explain the complexity of FOXA1 regulated genes in different cells. FOXA1's role in transcriptional repression is likely associated with its binding to repressors or modulators. We found that there was reduced binding of FOXA1 interacting co-repressors, including TLE3, NFIC and HDAC7 to FOXA1. TLE3 is a repressor that was found to associate with Wnt/β-Catenin driven EMT (44). FOXA1 was shown to recruit TLE3 to specific genomic target sites to elicit transcriptional repression. NFIC, which is involved in EMT regulation (45), was found to interact with FOXA1 to regulate the expression of prostate-specific genes (22). FOXA1 also interacts with HDAC7 that regulates N-COR/SMRT co-repressor complex recruitment (21). We have shown that these repressors contributed to FOXA1's ability to suppress the expression of invasion genes. Our studies further provide mechanistic insights on how FOXA1 represses invasion and how JQ1 activates invasion through the inhibition of FOXA1. Our results have shown, for the first time,

that JQ1 interacts with FOXA1 and disrupts FOXA1's ability to bind to repressors, hampering its repressor activity and allowing the expression of FOXA1 repressed invasion genes. We further showed that JQ1 reduced the stability of TLE3, HDAC7 and NFIC in prostate cancer cells. The destabilization of the repressors by JQ1 could be due either to disturbance of their interactions with FOXA1, which stabilize them in cellular environment, or through other mechanisms.

Taken together, our results indicate that JQ1 inactivates FOXA1 repressive activity, through direct binding to FOXA1 and disrupting the interactions between FOXA1 and its co-repressors, to promote prostate cancer invasion. This novel finding reveals that perturbation of FOXA1 activity by JQ1 may introduce an unexpected effect of JQ1 on cancer, especially in FOXA1 related cancers like prostate, breast and pancreatic cancer. It raises the possibility that combination treatment strategies, such as BMP inhibition, could be used to overcome the potential metastatic promoting effect of JQ1.

Methods

Cell lines, culturing condition and transfection

LNCaP, 22Rv1, C4-2, PC3 and 293T cells were purchased from ATCC and maintained in the Tissue and Cell Culture Core Facility at Baylor College of Medicine. Cells were cultured in RPMI 1640 medium (11875093, ThermoFisher, Waltham, MA) supplemented with 10% FBS (F2442, Sigma-Aldrich, Saint Louis, MO). LNCaP-abl cell line was obtained from Zoran Culig (Medical University of Innsbruck, Innsbruck, Austria) and maintained in RPMI 1640 medium supplemented with 10% charcoal stripped FBS (F6765, Sigma-Aldrich, Saint Louis, MO). The authenticity of all cell lines was verified in the last 6 months. Cell transfection was performed using Lipofectamine 2000 (11668019, ThermoFisher, Waltham, MA) for vectors and

Lipofectamine RNAiMAX (13778075, ThermoFisher, Waltham, MA) for siRNAs according to the manufacturer's instructions.

Chemicals

(-)-JQ1 (1268524-71-5, Cayman Chemical, Ann Arbor, MI), JQ1 (SML0974, Sigma-Aldrich, Saint Louis, MO), I-BET762 (SML1272, Sigma-Aldrich, Saint Louis, MO), OTX015 (202590-98-5, Cayman Chemical, Ann Arbor, MI), I-BET151 (SML0666, Sigma-Aldrich, Saint Louis, MO), LDN-212854 (SML0965, Sigma-Aldrich, Saint Louis, MO) were used.

Cell proliferation assay

Cells were seeded in 96-well plates at 1000-3000 cells per well. JQ1 was added the following day. After 96 hours of incubation, cell viability was assessed by CellTiter-Glo assay (G9241, Promega, Madison, WI). Cell proliferation was measured by CellTiter 96® AQueous One Solution Cell Proliferation Assay (G3582, Promega, Madison, WI). The value was measured at 490 nm using a Multiskan™ FC Microplate Photometer (Thermo Scientific, Waltham, MA) and normalized.

Transwell invasion assay

Cells were treated with JQ1 for 72 hours. 2×10^5 LNCaP, 2×10^5 LNCaP-abl, 0.5×10^5 22Rv1 and 1×10^5 C4-2 cells were seeded with serum-free medium in a transwell chambers pre-coated with Matrigel (354483, BD Biosciences, Franklin Lakes, NJ). Medium with 10% FBS was added in the lower chamber. JQ1 was added to both upper and lower chamber. After 24 hours (22Rv1) or 48 hours (LNCaP, LNCaP-abl and C4-2), cells were fixed with methanol. The non-invading cells were gently removed and invaded cells on the lower side of the chamber were stained with crystal violet, photographed and counted.

Focal adhesion measurement

Cells were treated with JQ1 for 72 hours, then seeded on a fibronectin coated plate for 6 hours. Immunofluorescence assay using paxillin antibody (ab32084, Abcam, Cambridge, UK) was performed to indicate focal adhesion. Cells were fixed with 4% PFA with 0.1% TritonX-100 for 10 minutes, then washed and blocked with PBS with 1% BSA and 0.2% TritonX-100. Cells were incubated with primary antibody (1:100 dilution in PBS with 1% BSA and 0.2% TritonX-100) overnight at 4℃. Further incubated with secondary antibody (A11002, ThermoFisher, Waltham, MA 1:1000 dilution) at room temperature for 1 hour. Focal adhesion number per cell was calculated using ImageJ software.

siRNA transfection

Cells were transfected with siRNA for 72 hours. siRNA targeting sequences are shown in Supplemental Table 1.

RNA-sequencing and GSEA analysis

LNCaP cells were treated with 200 nM JQ1 for 72 hours, and total RNA was extracted for RNA- sequencing analysis. The sequencing was done by EA Q2 Solutions (Morrisville, USA). The sequencing data was deposited in NCBI GEO database (GSE139230). Upregulated and downregulated genes were generated by filtering with fold change $Log_2 0.6$ as cut off. GSEA was performed using GSEA JAVA program. NES (Normalized Enrichment Score) and FDR (False Discovery Rate) q values were shown.

RNA isolation and q-RT-PCR

Total RNA was extracted from cells using Trizol reagent (15596018, ThermoFisher, Waltham, MA). cDNA was synthesized using Thermo Scientific™ Maxima™ First Strand cDNA Synthesis Kit (FERK1641, ThermoFisher, Waltham, MA). Real-time PCR was performed with FastStart Universal SYBR Green Master (4913850001, Roche, Basel, Switzerland) on a

StepOnePlus Real-Time PCR system (Applied Biosystems, Waltham, MA). Relative mRNA levels were normalized to ACTB. All primers were synthesized by Sigma Aldrich. The primer sequences are shown in Supplemental Table 2.

Western blot assay

Total proteins were extracted from cells following standard protocol. Protein concentration was measured using the BCA protein assay kit (23228, ThermoFisher, Waltham, MA). Protein samples were separated by SDS-PAGE and transferred onto nitrocellulose membrane (1620112, Bio-Rad, Hercules, CA). The membrane was incubated for 30 minutes in blocking buffer (TBST with 5% non-fat dry milk), followed by overnight incubation at 4 °C with the primary antibody. Membrane was then incubated with horseradish peroxidase (HRP)-conjugated secondary antibodies (7074 or 7076, Cell Signaling, Danvers, MA) for 1 hour. The signals were visualized with SuperSignal™ West Dura Extended Duration Substrate (34075, ThermoFisher, Waltham, MA). The primary antibodies used in this study were as follows: FOXA1 (ab23738, Abcam, Cambridge, UK), GAPDH (SC-25778 HRP, Santa Cruz, Dallas, TX), c-Myc (5605, Cell Signaling, Danvers, MA), Smad1 (6944, Cell Signaling, Danvers, MA), Smad5 (9517, Cell Signaling, Danvers, MA), p-Smad1/5 (9516, Cell Signaling, Danvers, MA), p-AKT (4060, Cell Signaling, Danvers, MA), AKT (9272, Cell Signaling, Danvers, MA), TLE3 (11372-1-AP, Proteintech, Wuhan, Hubei, P.R.C), HDAC7 (A301-384A-T, Bethyl, Montgomery, TX), NFIC (A303-123A-T, Bethyl, Montgomery, TX), Luciferase (ab21176, Abcam, Cambridge, UK), AR (5153, Cell Signaling, Danvers, MA).

Cellular thermal shift assay (CETSA)

The CETSA assay was done by the standard protocol (46). LNCaP cells were treated with 10 μM JQ1 for 1 hour. Cells were suspended in PBS with protease inhibitors, heated in indicated temperature for 3 minutes, and immediately snap-frozen. Samples were subjected to two

freeze-thaw cycles and centrifuged. Supernatants were collected and western blot assays were performed.

Pull down assay

Cells were lysed in IP buffer (20 mM Tris pH7.5, 150 mM NaCl, 1% Trion X-100, 1 mM EDTA, protease inhibitor). Biotinylated JQ1 (Biotin-JQ1) was generated through Cu(I)-catalyzed Azide Alkyne Click Chemistry reaction (CuAAC) (47). Briefly, 100 μM JQ1–PA (6589, Tocris, Bristol, UK), 200μM Biotin-azide (762024, Sigma-Aldrich, Saint Louis, MO), 4 mM CuSO4, 5 mM (+)-Sodium L-ascorbate (11140, Sigma-Aldrich, Saint Louis, MO) were incubated for 1 hour, followed by 1-hour incubation with Streptavidin-coupled Dynabeads (65601, ThermoFisher, Waltham, MA). Biotin-JQ1 or control compound (Biotin-azide) loaded beads were washed and incubated with cell lysate or purified FOXA1 protein (ab98301, Abcam, Cambridge, UK) for 4 hours at 4℃. Beads were washed by IP buffer, resuspended in loading buffer and boiled at 95℃ for 5 min for separation of the protein and beads. Samples were then analyzed by western blot.

Immunoprecipitation

Cells were treated with 10 μM JQ1 for 8 hours and harvested. Lysis buffer (10 mM HEPES pH 7.9, 10 mM KCl, 1.5 mM MgCl2, 1 mM EDTA, 0.5 mM DTT with protease inhibitor) was used to isolate cell nucleus. Cell nuclei were lysed in IP buffer (20 mM Tris pH7.5, 150 mM NaCl, 1% Trion X-100, 1 mM EDTA, protease inhibitor). After pre-clearing with protein G Dynabeads (10003D, ThermoFisher, Waltham, MA) for 1 hour, lysates were incubated with protein G Dynabeads preloaded with FOXA1 antibody (A305-249A, Bethyl, Montgomery, TX) overnight at 4℃. Beads were washed three times in IP buffer and resuspended in loading buffer and boiled at 95℃ for 5 min for separation of the protein and beads. Samples were then analyzed by western blot.

Mouse metastasis assay

All experiments were approved by the Animal Center for Comparative Medicine at Baylor College of Medicine. 8-week-old male SCID mice (NOD-CB17 *Prkdc*$^{SCID/J}$, stock number 001303) were purchased from The Jackson Laboratory (Bar Harbor, Maine). 22Rv1-luciferase and C4-2-luciferase cells were generated by lentivirus induced luciferase overexpression from pCDH-CMV-Luc2-T2A-tGFP-EF1-hygro. 1.5×10^6 22Rv1-luciferase or 4×10^6 C4-2-luciferase cells were injected into mice through the tail vein. The following day, mice were treated daily with 10 mg/kg JQ1 intraperitonially. After 7 weeks, bioluminescence was measured by IVIS system after intraperitoneal injection of luciferin (LUCK-1G, Gold Biotechnology, St Louis MO).

Mice of prostate cancer mouse models (Probasin-Cre driven *Pten* null mice, Pb-Cre;*Pten*$^{fl/fl}$) that fully backcrossed onto C57/BL6 background were maintained in our laboratory as previously described (48). Male mice of about 18 weeks old were treated daily with 10 mg/kg JQ1 intraperitonially for 7 weeks. Draining lumbar lymph nodes of mice were collected for immunohistochemistry assay to measure AR positive cells.

Immunohistochemistry assay

Immunohistochemistry was done as described previously (49). Primary AR antibody (ab133273, Abcam, Cambridge, UK, 1:500 dilution) was incubated overnight at 4 ℃, and secondary antibody (711-066-152, Jackson ImmunoResearch, West Grove, PA, 1:500 dilution) was incubated for 1 h at room temperature.

Chromatin Immunoprecipitation qPCR (ChIP-qPCR) assays

Chromatin immunoprecipitation assays were performed using Magna ChIP A/G kit from Millipore according to the manufacturer's protocol. FOXA1 (ab23738, Abcam, Cambridge, UK), TLE3 (11372-1-AP, Proteintech, Wuhan, Hubei, P.R.C), NFIC (A303-123A-T, Bethyl,

Montgomery, TX), HDAC7 (PA5-29937, ThermoFisher, Waltham, MA), and corresponding control IgG antibodies were used. The quantitative real-time PCR assays were carried out on chromatin samples prepared above. Primer sequences are shown in Supplemental Table 3.

Statistics

The statistical analyses were performed using Origin 2017 (Northampton, USA), and data were presented as dot plots, with the mean ± SD (standard deviation) indicated. Unpaired two tailed Student's t test was used for 2 group comparison. One-way analysis of variance (ANOVA) was used for comparison among multiple groups with one independent variable followed by post hoc Tukey's multiple comparisons test. Two-way analysis of variance (ANOVA) was used for comparison among multiple groups with two independent variables followed by Sidak's multiple comparisons test. Kaplan-Meier survival curve was analyzed by log rank test. The difference was regarded as significant when $P<0.05$. All experiments were repeated 2–4 times.

Study approval

All animal experimental procedures were reviewed and approved by the IACUC of Baylor College of Medicine, and all experiments were performed in compliance with the institutional guidelines of Baylor College of Medicine.

Author contributions

LMW, SYT, and MJT conceptualized and designed the study. LMW performed and analyzed the experiments. LMW and MFX completed cell assays and coimmunoprecipitation studies. CYK assisted with in vivo studies. LMW, SYT, and MJT wrote, discussed, and edited the manuscript.

Acknowledgements

We thank Dr. Li-Yuan Yu-Lee and Jodie R. Hebert for editorial assistance. We appreciate the technical support of Pei Li and Guannu Xu. We also thank the Tissue Culture Core of Molecular and Cellular Biology Department, the Cell-Based Assay Screening Service Core, and the Genetically Engineered Mouse Core for their assistance. This work was supported by grants from CPRIT RP150648 and NIH HL114539.

References

1. Nevedomskaya, E., Baumgart, S.J., and Haendler, B. 2018. Recent Advances in Prostate Cancer Treatment and Drug Discovery. *Int J Mol Sci* 19.
2. Karantanos, T., Corn, P.G., and Thompson, T.C. 2013. Prostate cancer progression after androgen deprivation therapy: mechanisms of castrate resistance and novel therapeutic approaches. *Oncogene* 32:5501-5511.
3. Rathkopf, D., and Scher, H.I. 2013. Androgen receptor antagonists in castration-resistant prostate cancer. *Cancer J* 19:43-49.
4. Lin, T.H., Izumi, K., Lee, S.O., Lin, W.J., Yeh, S., and Chang, C. 2013. Anti-androgen receptor ASC-J9 versus anti-androgens MDV3100 (Enzalutamide) or Casodex (Bicalutamide) leads to opposite effects on prostate cancer metastasis via differential modulation of macrophage infiltration and STAT3-CCL2 signaling. *Cell Death Dis* 4:e764.
5. Lin, T.H., Lee, S.O., Niu, Y., Xu, D., Liang, L., Li, L., Yeh, S.D., Fujimoto, N., Yeh, S., and Chang, C. 2013. Differential androgen deprivation therapies with anti-androgens casodex/bicalutamide or MDV3100/Enzalutamide versus anti-androgen receptor ASC-J9(R) Lead to promotion versus suppression of prostate cancer metastasis. *J Biol Chem* 288:19359-19369.
6. Wang, C., Peng, G., Huang, H., Liu, F., Kong, D.P., Dong, K.Q., Dai, L.H., Zhou, Z., Wang, K.J., Yang, J., et al. 2018. Blocking the Feedback Loop between Neuroendocrine Differentiation and Macrophages Improves the Therapeutic Effects of Enzalutamide (MDV3100) on Prostate Cancer. *Clin Cancer Res* 24:708-723.
7. Yang, Z., Yik, J.H., Chen, R., He, N., Jang, M.K., Ozato, K., and Zhou, Q. 2005. Recruitment of P-TEFb for stimulation of transcriptional elongation by the bromodomain protein Brd4. *Mol Cell* 19:535-545.
8. Shi, J., Wang, Y., Zeng, L., Wu, Y., Deng, J., Zhang, Q., Lin, Y., Li, J., Kang, T., Tao, M., et al. 2014. Disrupting the interaction of BRD4 with diacetylated Twist suppresses tumorigenesis in basal-like breast cancer. *Cancer Cell* 25:210-225.
9. Liu, W., Ma, Q., Wong, K., Li, W., Ohgi, K., Zhang, J., Aggarwal, A., and Rosenfeld, M.G. 2013. Brd4 and JMJD6-associated anti-pause enhancers in regulation of transcriptional pause release. *Cell* 155:1581-1595.
10. Stathis, A., and Bertoni, F. 2018. BET Proteins as Targets for Anticancer Treatment. *Cancer Discov* 8:24-36.
11. Asangani, I.A., Dommeti, V.L., Wang, X., Malik, R., Cieslik, M., Yang, R., Escara-Wilke, J., Wilder-Romans, K., Dhanireddy, S., Engelke, C., et al. 2014. Therapeutic targeting of BET bromodomain proteins in castration-resistant prostate cancer. *Nature* 510:278-282.

12. Filippakopoulos, P., Qi, J., Picaud, S., Shen, Y., Smith, W.B., Fedorov, O., Morse, E.M., Keates, T., Hickman, T.T., Felletar, I., et al. 2010. Selective inhibition of BET bromodomains. *Nature* 468:1067-1073.
13. Shu, S., Lin, C.Y., He, H.H., Witwicki, R.M., Tabassum, D.P., Roberts, J.M., Janiszewska, M., Huh, S.J., Liang, Y., Ryan, J., et al. 2016. Response and resistance to BET bromodomain inhibitors in triple-negative breast cancer. *Nature* 529:413-417.
14. Handoko, L., Kaczkowski, B., Hon, C.C., Lizio, M., Wakamori, M., Matsuda, T., Ito, T., Jeyamohan, P., Sato, Y., Sakamoto, K., et al. 2018. JQ1 affects BRD2-dependent and independent transcription regulation without disrupting H4-hyperacetylated chromatin states. *Epigenetics*:1-22.
15. Kurimchak, A.M., Shelton, C., Duncan, K.E., Johnson, K.J., Brown, J., O'Brien, S., Gabbasov, R., Fink, L.S., Li, Y., Lounsbury, N., et al. 2016. Resistance to BET Bromodomain Inhibitors Is Mediated by Kinome Reprogramming in Ovarian Cancer. *Cell Rep* 16:1273-1286.
16. Andrieu, G.P., and Denis, G.V. 2018. BET Proteins Exhibit Transcriptional and Functional Opposition in the Epithelial-to-Mesenchymal Transition. *Mol Cancer Res* 16:580-586.
17. Chan, S.C., Selth, L.A., Li, Y., Nyquist, M.D., Miao, L., Bradner, J.E., Raj, G.V., Tilley, W.D., and Dehm, S.M. 2015. Targeting chromatin binding regulation of constitutively active AR variants to overcome prostate cancer resistance to endocrine-based therapies. *Nucleic Acids Res* 43:5880-5897.
18. Kwon, A.T., Arenillas, D.J., Worsley Hunt, R., and Wasserman, W.W. 2012. oPOSSUM-3: advanced analysis of regulatory motif over-representation across genes or ChIP-Seq datasets. *G3 (Bethesda)* 2:987-1002.
19. Sekiya, T., and Zaret, K.S. 2007. Repression by Groucho/TLE/Grg proteins: genomic site recruitment generates compacted chromatin in vitro and impairs activator binding in vivo. *Mol Cell* 28:291-303.
20. Jangal, M., Couture, J.P., Bianco, S., Magnani, L., Mohammed, H., and Gevry, N. 2014. The transcriptional co-repressor TLE3 suppresses basal signaling on a subset of estrogen receptor alpha target genes. *Nucleic Acids Res* 42:11339-11348.
21. Malik, S., Jiang, S., Garee, J.P., Verdin, E., Lee, A.V., O'Malley, B.W., Zhang, M., Belaguli, N.S., and Oesterreich, S. 2010. Histone deacetylase 7 and FoxA1 in estrogen-mediated repression of RPRM. *Mol Cell Biol* 30:399-412.
22. Grabowska, M.M., Elliott, A.D., DeGraff, D.J., Anderson, P.D., Anumanthan, G., Yamashita, H., Sun, Q., Friedman, D.B., Hachey, D.L., Yu, X., et al. 2014. NFI transcription factors interact with FOXA1 to regulate prostate-specific gene expression. *Mol Endocrinol* 28:949-964.
23. Belkina, A.C., Nikolajczyk, B.S., and Denis, G.V. 2013. BET protein function is required for inflammation: Brd2 genetic disruption and BET inhibitor JQ1 impair mouse macrophage inflammatory responses. *J Immunol* 190:3670-3678.
24. Karagiannis, G.S., Pastoriza, J.M., Wang, Y., Harney, A.S., Entenberg, D., Pignatelli, J., Sharma, V.P., Xue, E.A., Cheng, E., D'Alfonso, T.M., et al. 2017. Neoadjuvant chemotherapy induces breast cancer metastasis through a TMEM-mediated mechanism. *Sci Transl Med* 9.
25. Karagiannis, G.S., Condeelis, J.S., and Oktay, M.H. 2018. Chemotherapy-induced metastasis: mechanisms and translational opportunities. *Clin Exp Metastasis* 35:269-284.
26. Kong, D., Ahmad, A., Bao, B., Li, Y., Banerjee, S., and Sarkar, F.H. 2012. Histone deacetylase inhibitors induce epithelial-to-mesenchymal transition in prostate cancer cells. *PLoS One* 7:e45045.
27. Miao, L., Yang, L., Li, R., Rodrigues, D.N., Crespo, M., Hsieh, J.T., Tilley, W.D., de Bono, J., Selth, L.A., and Raj, G.V. 2017. Disrupting Androgen Receptor Signaling Induces Snail-Mediated Epithelial-Mesenchymal Plasticity in Prostate Cancer. *Cancer Res* 77:3101-3112.
28. Singh, A., and Settleman, J. 2010. EMT, cancer stem cells and drug resistance: an emerging axis of evil in the war on cancer. *Oncogene* 29:4741-4751.

29. Darby, S., Cross, S.S., Brown, N.J., Hamdy, F.C., and Robson, C.N. 2008. BMP-6 over-expression in prostate cancer is associated with increased Id-1 protein and a more invasive phenotype. *J Pathol* 214:394-404.
30. Haudenschild, D.R., Palmer, S.M., Moseley, T.A., You, Z., and Reddi, A.H. 2004. Bone morphogenetic protein (BMP)-6 signaling and BMP antagonist noggin in prostate cancer. *Cancer Res* 64:8276-8284.
31. Fong, C.Y., Gilan, O., Lam, E.Y., Rubin, A.F., Ftouni, S., Tyler, D., Stanley, K., Sinha, D., Yeh, P., Morison, J., et al. 2015. BET inhibitor resistance emerges from leukaemia stem cells. *Nature* 525:538-542.
32. Shang, Y., Cai, X., and Fan, D. 2013. Roles of epithelial-mesenchymal transition in cancer drug resistance. *Curr Cancer Drug Targets* 13:915-929.
33. DeGraff, D.J., Grabowska, M.M., Case, T.C., Yu, X., Herrick, M.K., Hayward, W.J., Strand, D.W., Cates, J.M., Hayward, S.W., Gao, N., et al. 2014. FOXA1 deletion in luminal epithelium causes prostatic hyperplasia and alteration of differentiated phenotype. *Lab Invest* 94:726-739.
34. Zhao, Y., Tindall, D.J., and Huang, H. 2014. Modulation of androgen receptor by FOXA1 and FOXO1 factors in prostate cancer. *Int J Biol Sci* 10:614-619.
35. Sahu, B., Laakso, M., Ovaska, K., Mirtti, T., Lundin, J., Rannikko, A., Sankila, A., Turunen, J.P., Lundin, M., Konsti, J., et al. 2011. Dual role of FoxA1 in androgen receptor binding to chromatin, androgen signalling and prostate cancer. *EMBO J* 30:3962-3976.
36. Augello, M.A., Hickey, T.E., and Knudsen, K.E. 2011. FOXA1: master of steroid receptor function in cancer. *EMBO J* 30:3885-3894.
37. Robinson, J.L., Hickey, T.E., Warren, A.Y., Vowler, S.L., Carroll, T., Lamb, A.D., Papoutsoglou, N., Neal, D.E., Tilley, W.D., and Carroll, J.S. 2014. Elevated levels of FOXA1 facilitate androgen receptor chromatin binding resulting in a CRPC-like phenotype. *Oncogene* 33:5666-5674.
38. Song, Y., Washington, M.K., and Crawford, H.C. 2010. Loss of FOXA1/2 is essential for the epithelial-to-mesenchymal transition in pancreatic cancer. *Cancer Res* 70:2115-2125.
39. Huang, J.Z., Chen, M., Zeng, M., Xu, S.H., Zou, F.Y., Chen, D., and Yan, G.R. 2016. Down-regulation of TRPS1 stimulates epithelial-mesenchymal transition and metastasis through repression of FOXA1. *J Pathol* 239:186-196.
40. Xu, Y., Qin, L., Sun, T., Wu, H., He, T., Yang, Z., Mo, Q., Liao, L., and Xu, J. 2017. Twist1 promotes breast cancer invasion and metastasis by silencing Foxa1 expression. *Oncogene* 36:1157-1166.
41. Jagle, S., Busch, H., Freihen, V., Beyes, S., Schrempp, M., Boerries, M., and Hecht, A. 2017. SNAIL1-mediated downregulation of FOXA proteins facilitates the inactivation of transcriptional enhancer elements at key epithelial genes in colorectal cancer cells. *PLoS Genet* 13:e1007109.
42. Kim, J., Jin, H., Zhao, J.C., Yang, Y.A., Li, Y., Yang, X., Dong, X., and Yu, J. 2017. FOXA1 inhibits prostate cancer neuroendocrine differentiation. *Oncogene* 36:4072-4080.
43. Jin, H.J., Zhao, J.C., Ogden, I., Bergan, R.C., and Yu, J. 2013. Androgen receptor-independent function of FoxA1 in prostate cancer metastasis. *Cancer Res* 73:3725-3736.
44. Liu, L., Zhang, Y., Wong, C.C., Zhang, J., Dong, Y., Li, X., Kang, W., Chan, F.K.L., Sung, J.J.Y., and Yu, J. 2018. RNF6 Promotes Colorectal Cancer by Activating the Wnt/beta-Catenin Pathway via Ubiquitination of TLE3. *Cancer Res* 78:1958-1971.
45. Lee, H.K., Lee, D.S., and Park, J.C. 2015. Nuclear factor I-C regulates E-cadherin via control of KLF4 in breast cancer. *BMC Cancer* 15:113.
46. Jafari, R., Almqvist, H., Axelsson, H., Ignatushchenko, M., Lundback, T., Nordlund, P., and Martinez Molina, D. 2014. The cellular thermal shift assay for evaluating drug target interactions in cells. *Nat Protoc* 9:2100-2122.
47. Tyler, D.S., Vappiani, J., Caneque, T., Lam, E.Y.N., Ward, A., Gilan, O., Chan, Y.C., Hienzsch, A., Rutkowska, A., Werner, T., et al. 2017. Click chemistry enables preclinical evaluation of targeted epigenetic therapies. *Science* 356:1397-1401.

48. Qin, J., Wu, S.P., Creighton, C.J., Dai, F., Xie, X., Cheng, C.M., Frolov, A., Ayala, G., Lin, X., Feng, X.H., et al. 2013. COUP-TFII inhibits TGF-beta-induced growth barrier to promote prostate tumorigenesis. *Nature* 493:236-240.
49. Wang, L., Xu, M., Qin, J., Lin, S.C., Lee, H.J., Tsai, S.Y., and Tsai, M.J. 2016. MPC1, a key gene in cancer metabolism, is regulated by COUPTFII in human prostate cancer. *Oncotarget* 7:14673-14683.

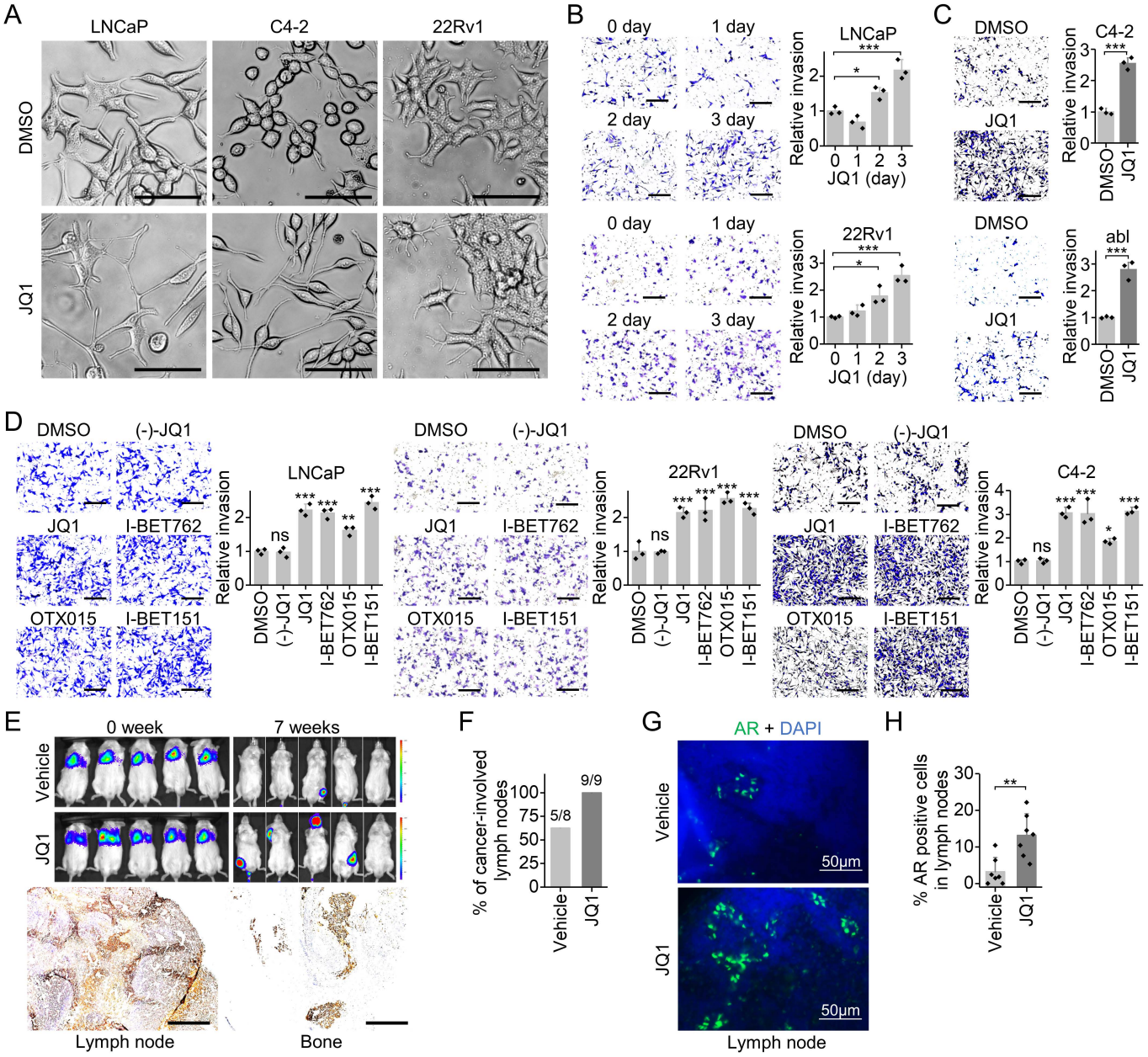

Figure 1. JQ1 promotes invasion of prostate cancer cells. (A) Representative photographs of cell morphology 2 days after 200 nM JQ1 treatment. Scale bar: 50 μm. (B) Cell invasion was measured at indicated days after 200 nM JQ1 treatment. Representative images of invasion were shown. Scale bar: 200 μm. n=3 per group, one-way ANOVA, *P<0.05, ***P<0.001. (C) Cell invasion was measured 3 days after 200 nM JQ1 treatment. Representative images of invasion were shown. Scale bar: 200 μm. n=3 per group, t test, ***p<0.001. (D) Cell invasion was measured 3 days after treatment with 200 nM indicated inhibitor. Representative images of invasion were shown. Scale bar: 200 μm. n=3 per group, one-way ANOVA, ns=p>0.05, *P<0.05, **P<0.01, ***P<0.001; compared to DMSO. (E) 22Rv1-Luc cells were injected into SCID mice through tail vein. 10 mg/kg JQ1 was given daily by intraperitoneal injection. Image was taken 7 weeks later. Metastatic sites with luciferase signal in different tissues were stained with AR antibody. Representative images of AR staining were shown. Scale bar: 400 μm. (F) Probasin-Cre Pten null mice of about 18 weeks old were given 10 mg/kg JQ1 for 7 weeks. Draining lumbar lymph nodes were collected for AR immunohistochemistry staining. % of cancer-involved lymph nodes (AR staining positive lymph nodes/total collected lymph nodes) was shown. (G) Representative AR staining in lymph nodes. Scale bar: 50 μm. (H) Quantitation of percent of AR positive cells in lymph node. n=8-9 per group, t test, **P<0.01.

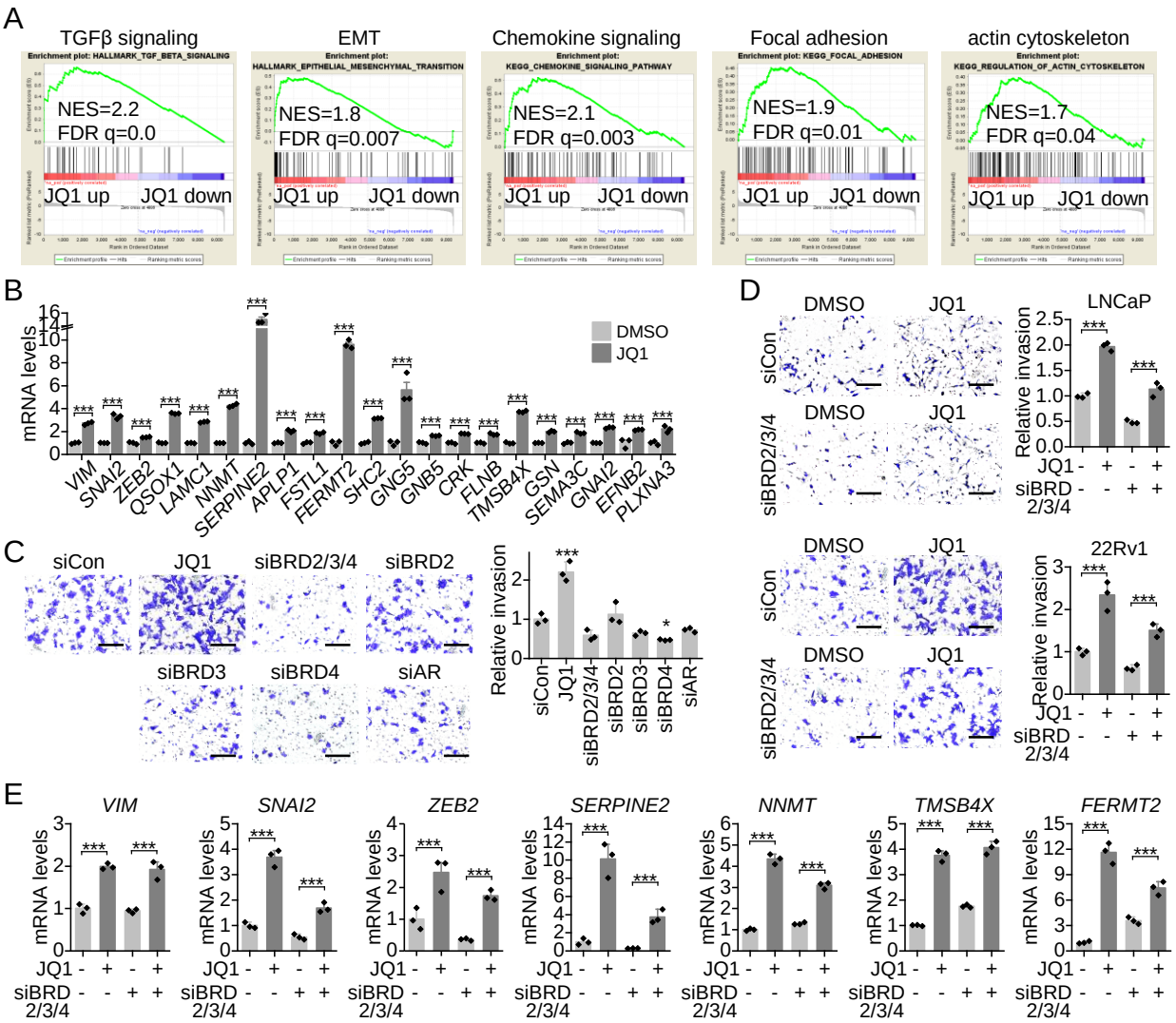

Figure 2. JQ1 activates invasion pathways. (A) GSEA showed activated invasion pathways by JQ1. (B) JQ1 promoted expression of invasion genes in the activated invasion pathways. n=3 per group, t test, ***P<0.001. (C) Cell invasion was measured 3 days after siRNA transfection. Representative images of invasion were shown. Scale bar: 200 μm. n=3 per group, one-way ANOVA, *P<0.05, ***P<0.001; compared to siCon (control siRNA). (D) JQ1 promoted invasion in the absence of BET proteins. Invasion was measured 3 days after JQ1 treatment and siRNA transfection. Representative images of invasion were shown. Scale bar: 200 μm. n=3 per group, two-way ANOVA, ***P<0.001. (E) JQ1 activated invasion genes in the absence of BET proteins. mRNA levels were measured 3 days after JQ1 treatment and siRNA transfection. n=3 per group, two-way ANOVA, ***P<0.001.

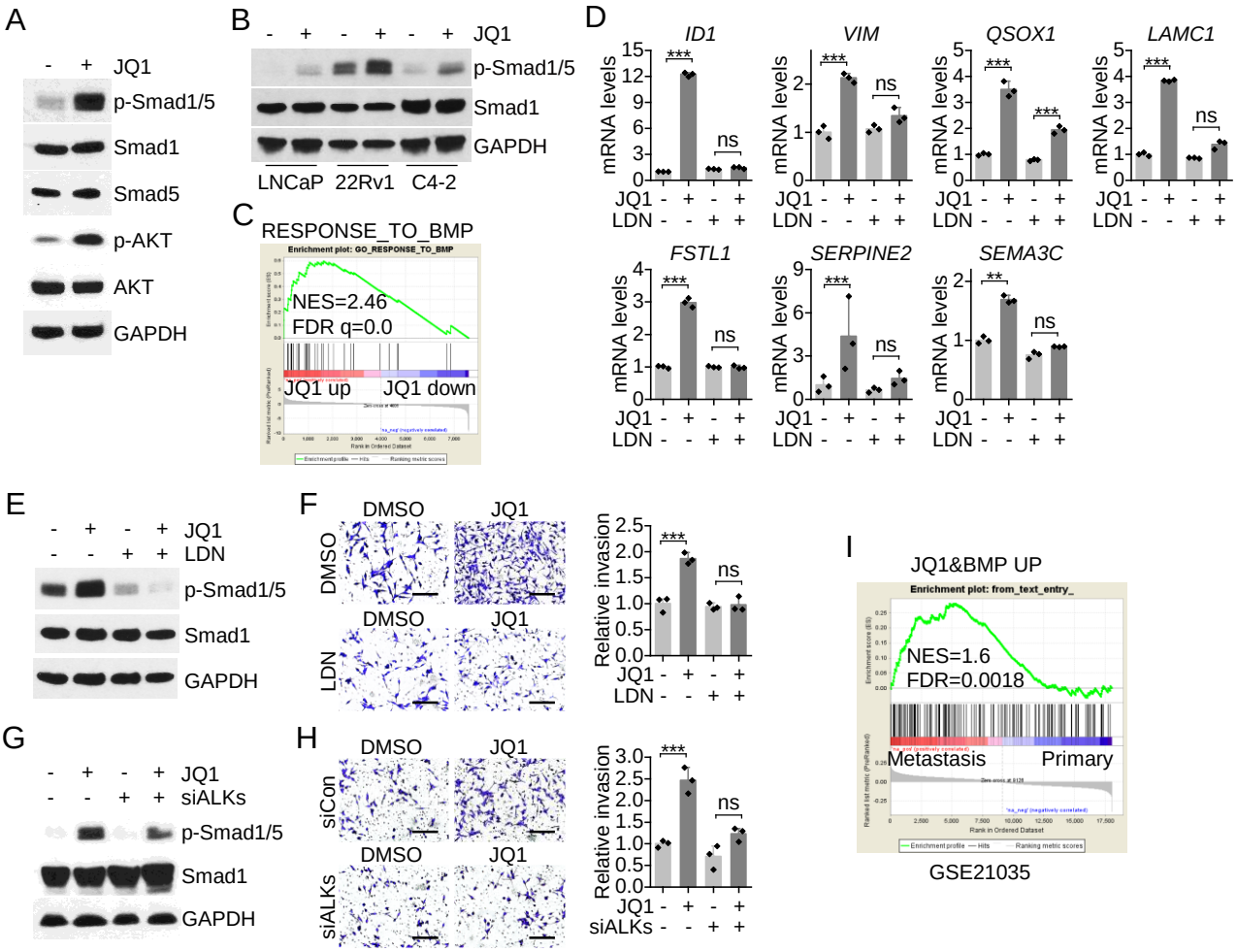

Figure 3. JQ1 activates BMP signaling. (A) Protein levels were measured in JQ1 treated LNCaP cells. (B) Phosphorylated Smad1/5 was measured in JQ1 treated cells. (C) GSEA showed that the response to BMP signature was activated by JQ1. (D) BMP signaling inhibitor LDN-212854 (LDN) impaired JQ1 induced upregulation of invasion genes. n=3 per group, two-way ANOVA, ns=p>0.05, ***P<0.001. (E) Indicated protein levels after LDN-212854 (LDN) and JQ1 treatment. (F) Cells were treated with 200 nM JQ1 and 2 μM LDN-212854 for 3 days and invasion was measured. Representative images of invasion were shown. Scale bar: 200 μm. n=3 per group, two-way ANOVA, ns=p>0.05, ***P<0.001. (G) Indicated protein levels after siALKs (siRNAs targeting ALK1, 2 and 3) transfection and JQ1 treatment. (H) Cells were transfected with siALKs, treated with JQ1 for 3 days, then invasion was measured. Representative images of invasion were shown. Scale bar: 200 μm. n=3 per group, two-way ANOVA, ns=p>0.05, ***P<0.001. (I) GSEA showed JQ1-activated BMP target gene signature was enriched in human metastatic prostate cancer tissues (GSE21035). JQ1 activated BMP target gene signature was generated through combining JQ1 upregulated genes and BMP positively regulated genes (GSE96914).

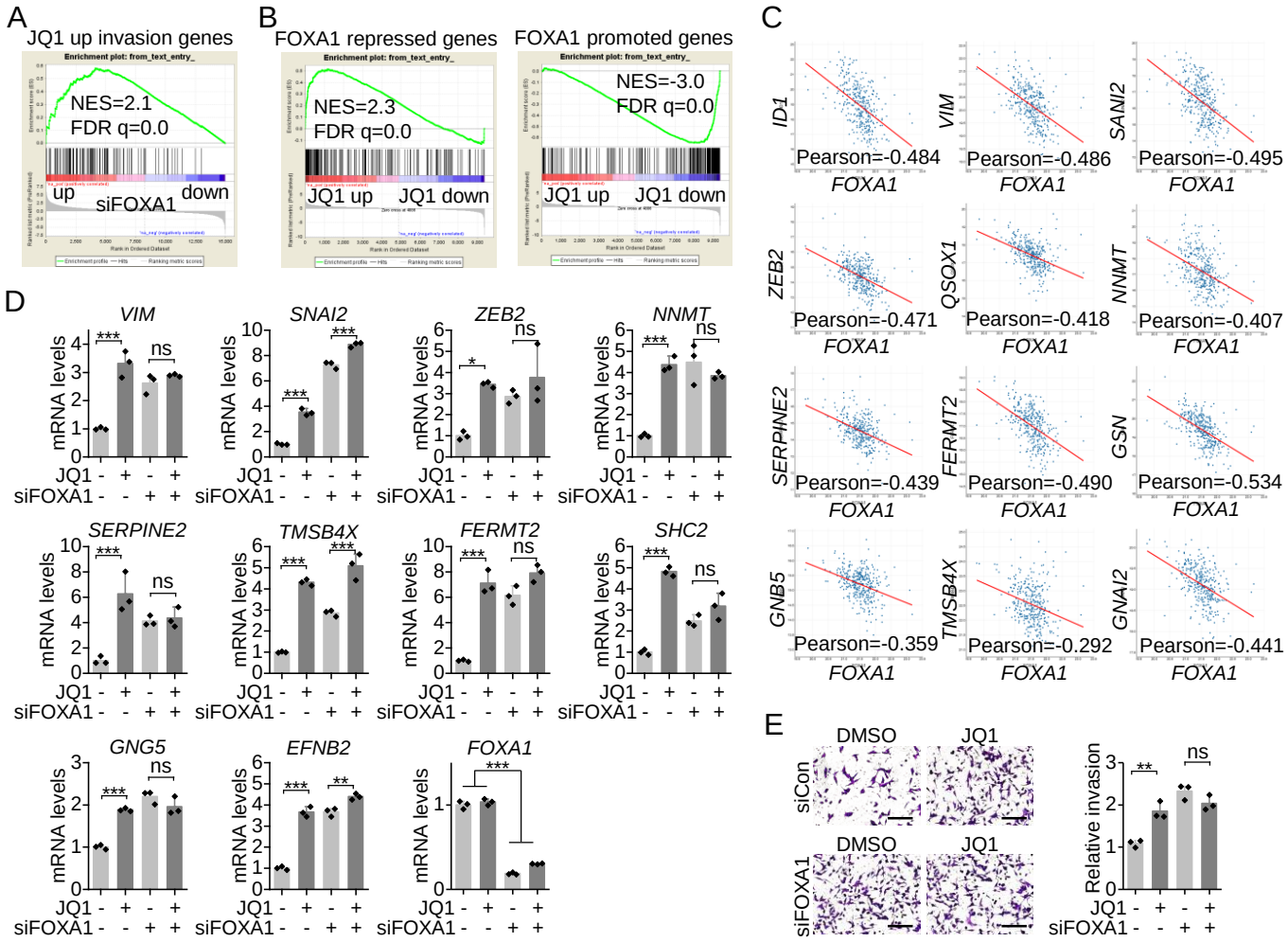

Figure 4. JQ1 represses FOXA1 to promote invasion. (A) GSEA showed JQ1-activated invasion genes were repressed by FOXA1 (GSE58309). (B) GSEA showed FOXA1 signature negatively enriched with JQ1 treatment. FOXA1 gene signature was generated by GSE58309. (C) FOXA1 negatively correlated with JQ1-activated invasion genes in patient prostate cancer tissues form the TCGA dataset. (D) FOXA1 knockdown impaired JQ1-induced upregulation of invasion genes. mRNA levels were measured 3 days after JQ1 treatment and siRNA transfection. n=3 per group, two-way ANOVA, ns=P>0.05, *P<0.05, **P<0.01, **P<0.001. (E) FOXA1 knockdown promoted cell invasion. Invasion was measured 3 days after JQ1 treatment and siRNA transfection. Representative images of invasion were shown. Scale bar: 200 μm. n=3 per group, two-way ANOVA, ns=P>0.05, **P<0.01.

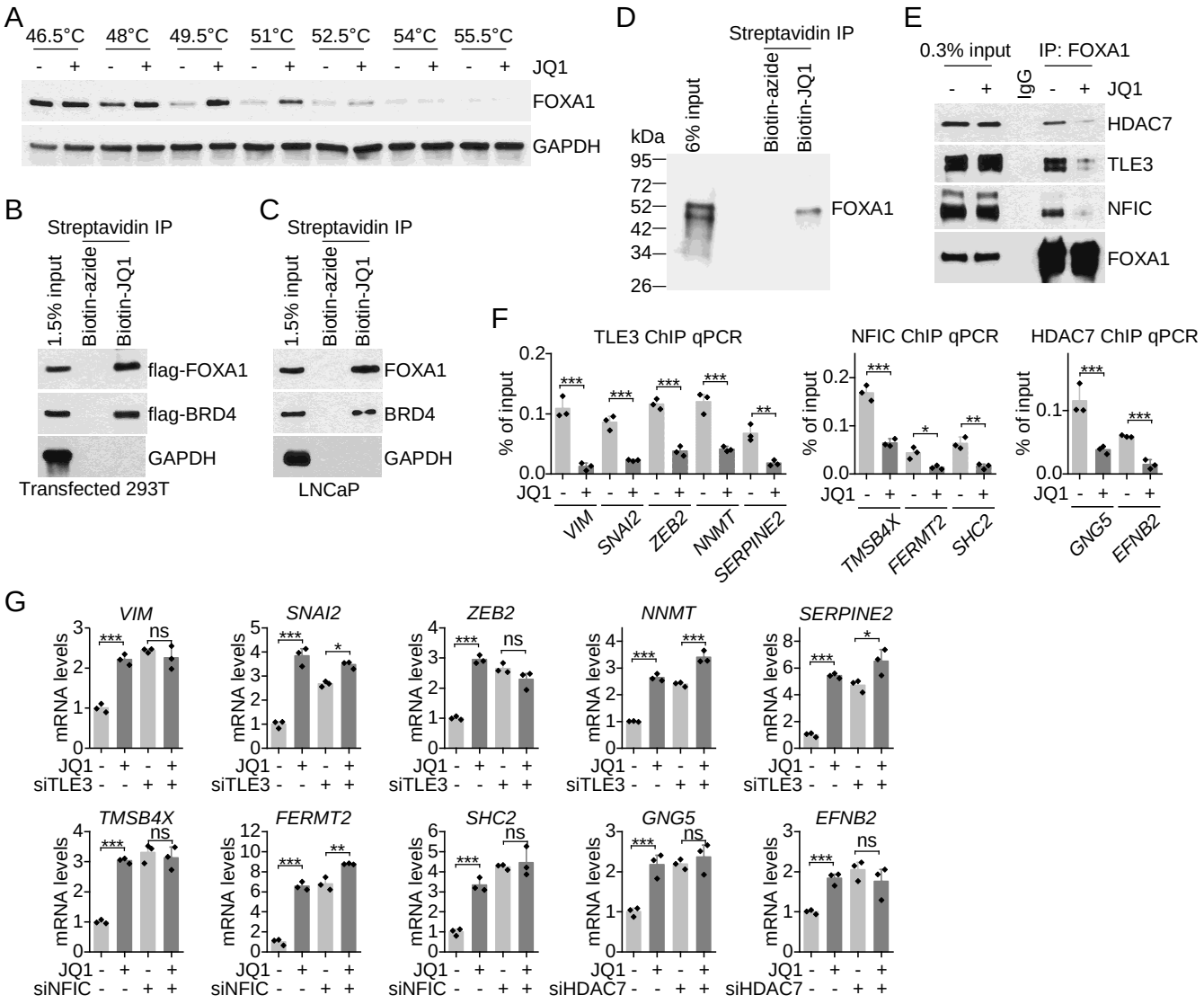

Figure 5. JQ1 interacts with FOXA1 to block associated repressor activity. (A) Cellular thermal shift assay (CETSA) was performed using LNCaP cells. (B) Biotin-JQ1 pull down assay using lysate of 293T cells that overexpressed with flag-FOXA1 and flag-BRD4. Biotin-azide was used as control. (C) Biotin-JQ1 pull down assay using LNCaP cell lysate. (D) Biotin-JQ1 pull down assay using FOXA1 recombinant protein. (E) LNCaP cells were treated with JQ1 for 8 hours. Immunoprecipitation was performed to measure FOXA1 binding to indicated proteins. (F) ChIP-qPCR assay of FOXA1 interacting repressors at FOXA1 binding sites on the promoter of JQ1-activated invasion genes. n=3 per group, t test, *P<0.05, **P<0.01, ***P<0.001. (G) FOXA1 interacting repressors regulated JQ1-activated invasion genes. n=3 per group, two-way ANOVA, ns=P>0.05, *P<0.05, **P<0.01, ***P<0.001.